Characterization, identification and life prediction of acoustic emission signals of tensile damage for HSR gearbox housing material

Ai Yibo, Zhang Yuanyuan, Cui Hao and Zhang Weidong
National Center for Materials Service Safety, University of Science and Technology Beijing, Beijing, China

Received 30 January 2023
Revised 3 February 2023
Accepted 3 February 2023

Abstract

Purpose – This study aims to ensure the operation safety of high speed trains, it is necessary to carry out nondestructive monitoring of the tensile damage of the gearbox housing material in rail time, yet the traditional tests of mechanical property can hardly meet this requirement.

Design/methodology/approach – In this study the acoustic emission (AE) technology is applied in the tensile tests of the gearbox housing material of an high-speed rail (HSR) train, during which the acoustic signatures are acquired for parameter analysis. Afterward, the support vector machine (SVM) classifier is introduced to identify and classify the characteristic parameters extracted, on which basis the SVM is improved and the weighted support vector machine (WSVM) method is applied to effectively reduce the misidentification of the SVM classifier. Through the study of the law of relations between the characteristic values and the tensile life, a degradation model of the gearbox housing material amid tensile is built.

Findings – The results show that the growth rate of the logarithmic hit count of AE signals and that of logarithmic amplitude can well characterize the stage of the material tensile process, and the WSVM method can improve the classification accuracy of the imbalanced data to above 94%. The degradation model built can identify the damage occurred to the HSR gearbox housing material amid the tensile process and predict the service life remains.

Originality/value – The results of this study provide new concepts for the life prediction of tensile samples, and more further tests should be conducted to verify the conclusion of this research.

Keywords HSR gearbox housing, Damage identification, Acoustic emission technology, Support vector machine, Weighted, Life prediction

Paper type Research paper

1. Introduction and literature review

As a key component of a high speed train, the reliability of the gearbox exerts direct impact to operation safety and may influence the entire railway transportation and its socioeconomic performance. The high-speed rail (HSR) gearbox housing represents an external protection structure and a key component that ensures the operation of the gearbox. The complex structure of the HSR gearbox housing is cast and installed onto the bogie in the form of nose suspension. The failure of the gearbox housing mainly takes place in modes of fatigue damage and tensile damage with the former caused by the operation-induced reciprocating

The research was supported by the National Natural Science Foundation of China (Grant No. U61273205).

Railway Sciences
Vol. 2 No. 2, 2023
pp. 225-242
Emerald Publishing Limited
e-ISSN: 2755-0915
p-ISSN: 2755-0907
DOI 10.1108/RS-01-2023-0007

oscillation of the gearbox housing and the latter caused by the partial static load of the gearbox housing and the accidental impact from external hard objects. The increase of the service mileage brings down the fatigue reliability of the gearbox housing (Wang, Zang, Qu, Li, & Dai, 2018), meaning that the tensile damage caused by external impact is more likely to happen. Therefore, it is of great significance to identify in real-time the nondestructive damage of the HSR gearbox housing and conduct life prediction, so as to ensure the operation safety of high speed trains.

Acoustic emission (AE) signals are very sensitive to the generation and expansion of material internal cracks as well as other defects. Given that such sensitivity is immune to the changes of materials, the approach is widely used to detect the existence and development of defects of in-service equipment. Roder, Guerrero-mata, and Colás (2003) studied the development of cracks in hard-faced AISI (American Iron and Steel Institute) type 304 stainless steel, but the study was based on destructive tests. Andreykiv, Skalsky, Serhiyenko, and Rudavsky (2010) used AE signals to determine the areas and spatial orientations of cracks of the aluminum alloy under tensile and torsion loads. However, only AE amplitude was considered in the crack calculation, overlooking the signal analysis. Hamdi, Duff, Simon, Plantier, Sourice, and Feuilloy (2013) realized the health monitoring of the AE mode structure in polymer composite materials using the Hilbert-Huang transform, but it is only suitable for composite materials. As a new real-time nondestructive testing method, the AE technology has been applied in recent studies of metal materials. Huang *et al.* (2017), by counting and analyzing the cumulative AE events amid metal fatigue damage process, identified the four different stages of the fatigue damage process of No. 45 steel with mechanical notches and proved that the kolmogorov entropy and correlation dimension of AE signals can be used as characteristic quantities for the severity of metal fatigue damage. Shi, Li, Wang, and Pan (2019) proposed an AE signal processing method using the wavelet packet energy spectrum to monitor and evaluate the severity of structural fatigue damage of materials in the early stage. Bhuiyan, Choudhury, Dahari, Nukman, and Dawal (2016) used AE sensors to measure the signal frequency of tool wear during metal cutting and identified that the frequency range of tool wear occurrences was 67–471 kHz. Li, Luo, Long, Chen, and Li (2016) integrated the time reversal focusing theory in the AE testing of steel plates and effectively improved the energy of the damage sound source signals. Through signal reconstruction and positioning display, the location of the damage sound source was accurately located.

In the application of AE technology, some researchers integrate AI (artificial intelligence) technologies for AE signal identification. Griffin, Shanbhag, Pereira, and Rolfe (2021) correlated the AE characteristics in the sheet metal stamping process with the flash wear. The training of the neural network helped realize the accurate classification of rolling wear of the stamping tools. Yao, Zhang, Ming, and Liu (2010) analyzed the AE signals of the gearbox both in normal state and in cracking fault state, during which the support vector machine (SVM) training samples were extracted, helping realize the fault detection of gear cracks. Wang, Zhu, Mao, and Huang (2010) integrated kernel principal component analysis (KPCA) and SVM to locate the crack source of hydroturbine blade according to AE signals. Melnikov, Averin, and Melnikova (2019) transformed the fuzzy clustering of AE pulses and resolved the classification of metal samples (deformation and nondeformation) with the help of neural network. The results determined the subpixel sampling of acoustic data on clusters and neural network learning algorithm for the automatic calculation of the characteristics of metals. However, at present, there are fewer studies about identification of tensile damage of the HSR gearbox housing material; therefore, in-depth research is vital for improving the accuracy of extraction and identification of damage characteristics.

Metal materials undergo four stages amid tensile, namely elastic, yield, plastic and fracture (Yoshida, Tokuyama, Yasuhara, & Nishino, 2012). The stress-strain curve of the HSR gearbox housing sample in the tensile process is shown in Figure 1. It can be seen that when

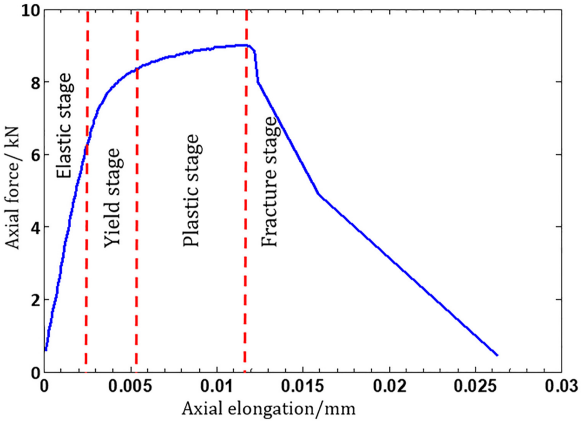

Figure 1.
Stress-strain curve of the gearbox housing amid tensile process

the deformation is in the elastic stage, the material can be restored to its original state upon the removal of the external force, therefore this stage is considered safe since it has little impact on service life of the material. Once the deformation of material enters the yield stage, irrecoverable deformation occurs within, greatly undermining its service reliability. This stage is considered as unsafe, that is to say, the remaining three stages in the material tensile process – yield, plastic and fracture – are classified as the early warning stages.

This paper takes the gearbox housing of a high speed train as the study object, and extracts characteristic values that effectively represent the damage stage of the material with the analysis of AE signals adopted by the equipped AE instrument amid the tensile test. Then, SVM and weighted support vector machine (WSVM) methods are adopted to learn and identify the AE signals, so as to identify the damage of material during the safe stage and early warning stage of the tensile process. The law of relation between the characteristic values of AE signals and the tensile life guide the prediction of the service life of the gearbox housing material remains, realizing its safety performance evaluation.

2. Methodology

2.1 AE technology

It is widely acknowledged that the deformation and the cracking development of materials under stress present important indicators for structural failure. AE, also known as stress wave emission, is defined as the phenomenon that transient elastic wave is generated by a sudden release of local energy within the material. As the elastic waves emitted from an AE source reach the material surface, displacement detectable to an AE sensor can be generated. The mechanical vibration of the material captured by the detector is converted into electrical signals, which are then amplified, processed and recorded.

According to modern plastic theory, dislocation and slip play a decisive role in the process of plastic deformation. Ideally, metal atoms are arranged in a certain order. However, the reality is that there are many defects in metals, and that dislocation is one of them, which is caused by the troubleshooting of positions by atoms. Under external stress, the dislocation moves on the slip plane, causing plastic deformation of the metal. The lattice dislocation moves from the low-energy position to another one, and vibrates at the new lattice position. The calculation results show that the high speed motion of the dislocation emits high-frequency AE signals of low amplitude, while the slow motion emits low-frequency signals of high amplitude. The signal energy of one dislocation is too low to be detected by the AE sensor with high sensitivity.

Therefore, it is assumed that many dislocations move simultaneously. It is estimated that when there is about 100 to 1,000 dislocations moving simultaneously, the AE sensor can receive continuous signals; and when hundreds to thousands of dislocations are moving simultaneously, the AE sensor can receive burst signals (Dong, 2007).

AE diagnosis of high sensitivity, capable of detecting the development of microcracks on the micrometer, is used to diagnose the generation and development of cracks caused by plastic deformation, fatigue and wear. The analysis of the AE signal parameters contributes to the classification of material damage states. The AE parameter analysis method is to analyze and interpret AE signals according to the waveform characteristics of AE signals. Common AE parameters include energy, ring count, duration, amplitude and effective voltage. The AE parameters selected are as follows.

(1) Energy

The energy measurement takes both amplitude and duration as the parameters to reflect the energy released by the AE source in the form of elastic waves. The energy E can be expressed as

$$E = \sum \left[\left(\frac{A}{G} \right)^2 - S^2 \right] \tag{1}$$

where

A – the amplitude of the point exceeding the threshold;

G – the gain;

S – the threshold.

(2) Ring count

The ring count is the number of pulses for the threshold ring. The sum exceeding the threshold in a specific time period is called the total ring count, and the sum exceeding the threshold per unit time is called the ring count rate. The ring count can directly reflect the intensity of the AE source. The ring count method is simple and widely used for AE monitoring, but it is greatly affected by the threshold.

(3) Hit count

A signal that exceeds the threshold and causes one channel to acquire data is called a hit, and the cumulative hit counts of the system are divided into the total count and the count rate. The hit count reflects the total number and frequency of AE activities and is generally used for the evaluation of AE activities.

(4) Amplitude

The amplitude refers to the maximum amplitude of the signal waveform, in dB. It is not subject to the threshold value and is related to the scale of the AE event. It can be used to directly judge the detectability of events.

2.2 AE data acquisition

A piece of high-strength aluminum alloy is cut from the HSR gearbox housing and is then processed into standard tensile samples using wire cutting. A total of 6 samples are selected. The dimensions of these samples are shown in Figure 2.

MTS-810 testing machine is used in the test. Both ends of the tensile sample are fixed on the testing machine. PCI-2 AE instrument and R15A sensor produced by PAC (physical acoustics company) (United States of America (USA)) are selected as the AE signal acquisition system. Vaseline is used as a coupling agent to connect the sensor with the sample. The sensor is fixed on the sample in order to avoid any loosening or falling-off.

The loading equipment of the testing machine applies a longitudinal tensile force which gradually increases until the sample fractured. Then, the test ended. During the whole process of the tensile test, the AE instrument continuously acquires AE signals and transmits them onto the computer workstation. The testing apparatus equipped with AE instrument is shown in Plate 1.

The loading rate of the loading equipment is 0.4 mm·min^{-1}, and the parameter settings of the AE signal acquisition system are shown in Table 1.

3. Characteristics and waveform of AE parameters

3.1 Preprocessing of acquired data

Although mechanical property data are recorded during the mechanical property test, the sampling time points cannot correspond to those of the AE hit. A close comparison shows that the number of mechanical property data sampling points is far less than that of AE hits, and that the variation of the mechanical property data tends to be mild. Therefore, it is necessary to resample the mechanical property data.

Mechanical property data are resampled by the reverse difference method.

Any two adjacent data sampled are assumed to be (x_n, y_n) and $(x_{n+1}, y_{n+1}), n = 1, 2\ldots$, and in (x'_n, y'_n), let $x_n < x'_n < x_{n+1}$, then the resampling value y is

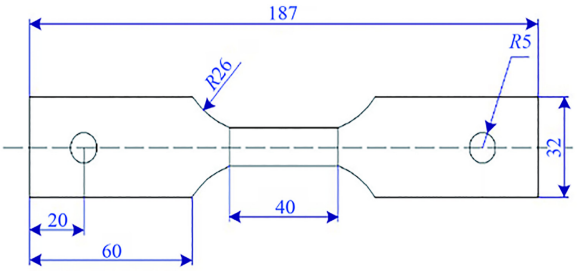

Figure 2.
Dimensions of tensile samples (Unit: mm)

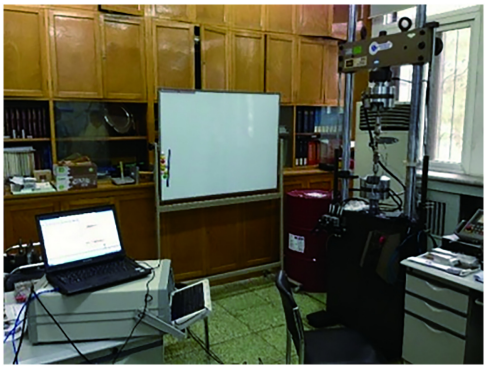

Plate 1.
Tensile testing apparatus equipped with AE instrument

$$y'_n = y_n \frac{(x_{n+1} - x'_n)}{s_n} + y_{n+1} \frac{(x'_n - x_n)}{s_n} \tag{2}$$

where $\frac{(x_{n+1} - x'_n)}{s_n} + \frac{(x'_n - x_n)}{s_n} = 1$

where s_n – the time interval between two adjacent sampling points.

3.2 Parameter characteristics

Based on what are obtained from AE signals and on the accumulation characteristics of the data required for analysis, 3 parameters, namely energy, ring count and hit count, are selected for analysis and processing. The relationships between the three parameters and the strain are shown in Figures 3–5, respectively.

Figure 3 shows that when the strain is less than 0.018, the cumulative energy count and the strain display an approximate linear relation, however as the strain goes beyond 0.018, the cumulative energy count has a large transition. This indicates that only a few AE signals are generated at low strain, while a large number of signals can be generated only when the sample enters the necking stage and finally fractures.

Table 1.
Parameters of AE signal acquisition system

Parameter	Value
Resonant frequency	150 kHz
Pregain amplifier	40 dB
Threshold	45 dB
Peak discrimination time (PDT)	300 μs
Hit discrimination time (HDT)	600 μs
Hit lock time (HLT)	1000 μs
Sampling frequency	1 MHz
Length of hit file	2 kB

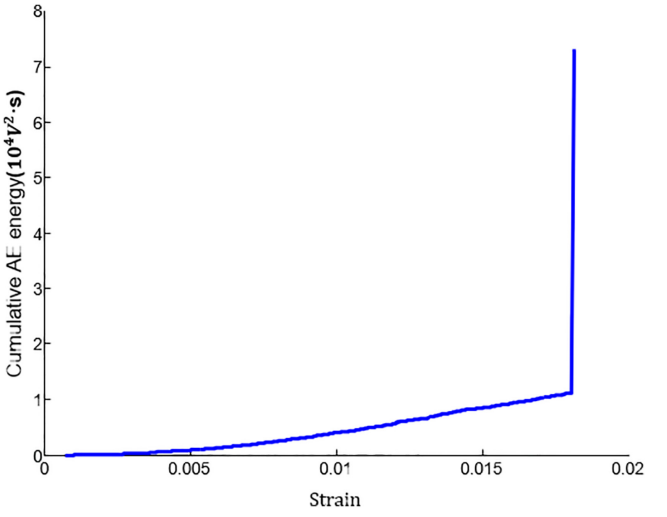

Figure 3.
Relationship between cumulative AE energy and strain

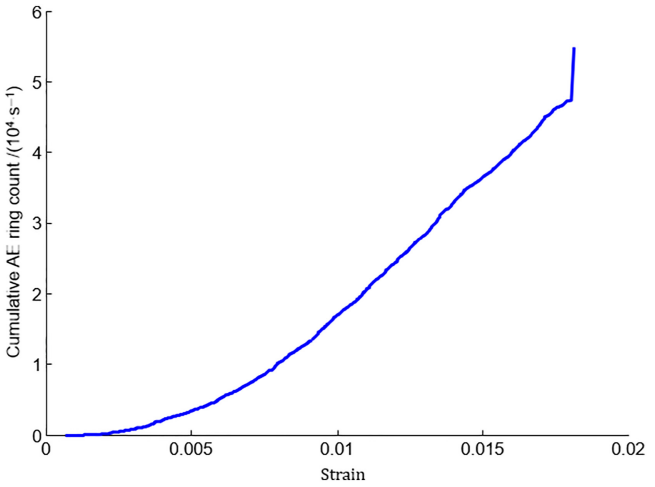

Figure 4.
Relationship between cumulative AE ring count and strain

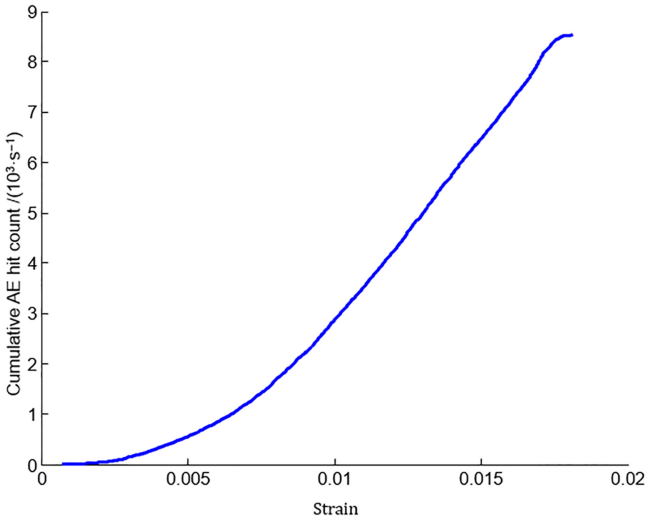

Figure 5.
Relationship between cumulative AE hit count and strain

Figure 4 shows that when the strain is less than 0.018, the cumulative ring count and the strain are in an approximate linear relation. When the strain is greater than 0.018, the ring count undergoes a large transition. This indicates that signal growth trend of AE ring count tends to be mild at low strain. The ring count increases rapidly only when the sample enters the necking stage and finally fractures.

Figure 5 shows that when the strain is less than 0.008, the cumulative AE hit count goes up yet very slowly, after which the two show an approximate linear relation. This indicates the signal growth of cumulative AE hit count tends to be moderate.

3.3 Waveform of AE hits

3.3.1 Time domain analysis. Theoretically, materials have limited or even no AE signals in the elastic deformation stage, however as the plastic deformation reaches a certain degree,

AE signals are generated. In the yield stage, AE signals increase sharply and the amplitude also increases; and when the deformation reaches the final fracture stage, large-amplitude AE signals appear.

In the tensile test of the gearbox housing, there are 2,048 sampling points for each AE hit with the sampling frequency being 1 MHz. See Figure 6 for the waveform curve of the AE hit with the maximum amplitude in the four stages (elastic deformation, plastic deformation, yield and fracture).

Figure 6 shows that the maximum amplitudes of AE hits are 0.09, 0.17, 0.27 and 0.065 V respectively for the four stages. From the elastic to the yield stage, the amplitude of AE signals increases but not in a significant way. From the yield to the fracture stage, the amplitude of AE signals decreases, indicating that although the amplitude does not increase in the tensile process of sample, the duration of hits goes up. Therefore, it can be known that the ring count, energy count and hit count all increase.

3.3.2 Frequency domain analysis. Given the transiency and the randomness of the AE signal, AE signals are classified as nonstationary random signals, composed of a series of signals with various frequencies and modes. Since transient and random signals vary with information such as time and frequency, the frequency structures need to be further analyzed.

The waveform of the AE hit with the maximum amplitude in Figure 6 is selected, and after Fourier transform, the amplitude-frequency curve as shown in Figure 7 is obtained.

It can be seen from Figure 7 that the peak frequencies of the four stages are 183, 153, 133 and 133 kHz respectively, and are relatively stable in each stage. Moreover, the frequency distribution in each stage is relatively uniform, and the energy is mainly concentrated in the range of 80-400 kHz.

4. Results of identification and analysis

4.1 Characteristics extraction

This paper looks into energy, ring count and amplitude as well as other AE parameters acquired during the tensile tests of the 6 samples as well as their changing patterns with the

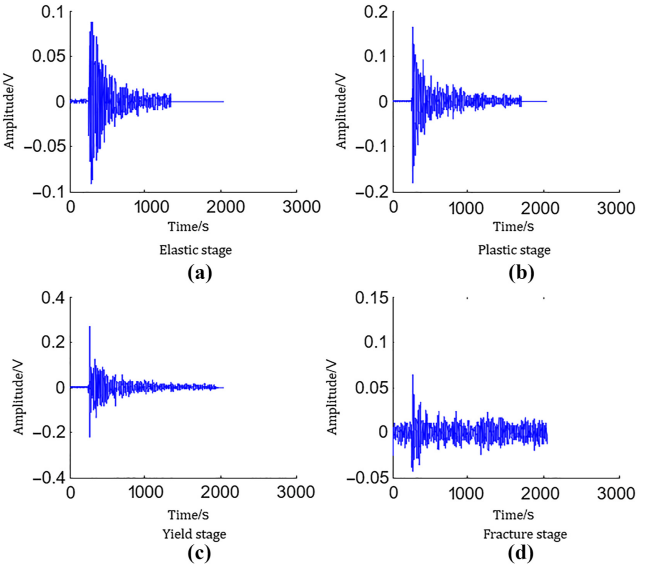

Figure 6.
Waveform of maximum AE hit in four stages of tensile test

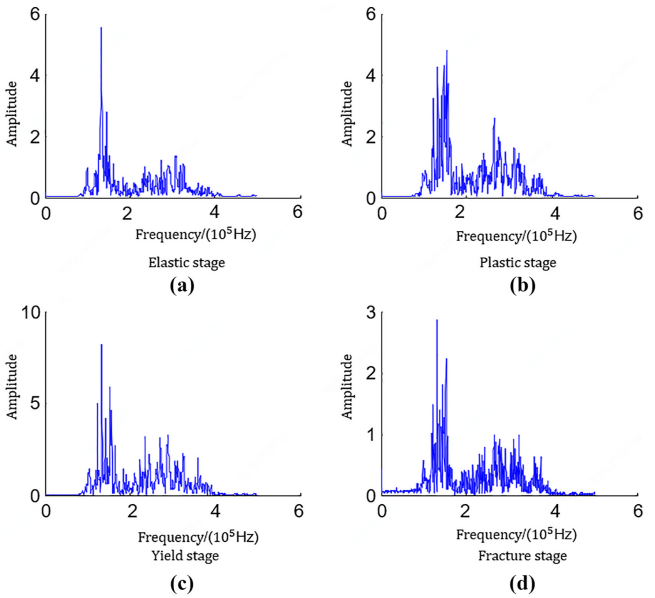

Figure 7.
Amplitude-frequency curve of maximum AE hit in four stages of tensile test

development of time. It takes sample 1 as an example, and the change curves of AE parameters are shown in Figure 8. The red dotted lines indicate the boundary line dividing the safe stage and early warning stage of the material (this approach is also used in the following figures).

Figure 8 shows that AE activities tend to occur in a more frequently manner, however, none of the 3 parameters shows obvious pattern and therefore cannot effectively characterizes the stage of the material.

In order to verify the increased frequency of AE activities, the growth rates of ring count, hit count and amplitude are calculated, and the logarithms of the calculated results are taken. Growth rate curves of logarithmic ring count, logarithmic amplitude and logarithmic hit count of each sample are shown in Figures 9–11, respectively.

It can be seen from Figure 9 that no obvious pattern is found in the growth rate of logarithmic ring count of sample 4 and 5. Although the curves fluctuate greatly, the change is not obvious around the boundary of the safe stage and the early warning stage. This indicates that the growth rate of logarithmic ring count is irrelevant to the stage of the sample. However, obvious patterns are picked up in the growth rate curves of logarithmic ring count of other samples, namely a monotonic increase. That being said, major fluctuations are noticed in samples 1 and 6.

Figure 10 shows that the growth rates of the logarithmic hit count of all sample are relatively obvious and consistent, namely a monotonic increase on the whole. When the sample is in the safe stage, the growth rates of logarithmic hit count are all below 0. After the sample entering the plastic stage, growth rates fluctuate around 0 and go up, and the values in the second half are obviously above 0.

Figure 11 shows that for each sample, apart from the variation range, the growth rate curve of logarithmic amplitude is similar to that of logarithmic hit count. When the sample is in the safe stage, values are all below 4, but after the sample entering the plastic stage, values fluctuate around 4 and start to increase.

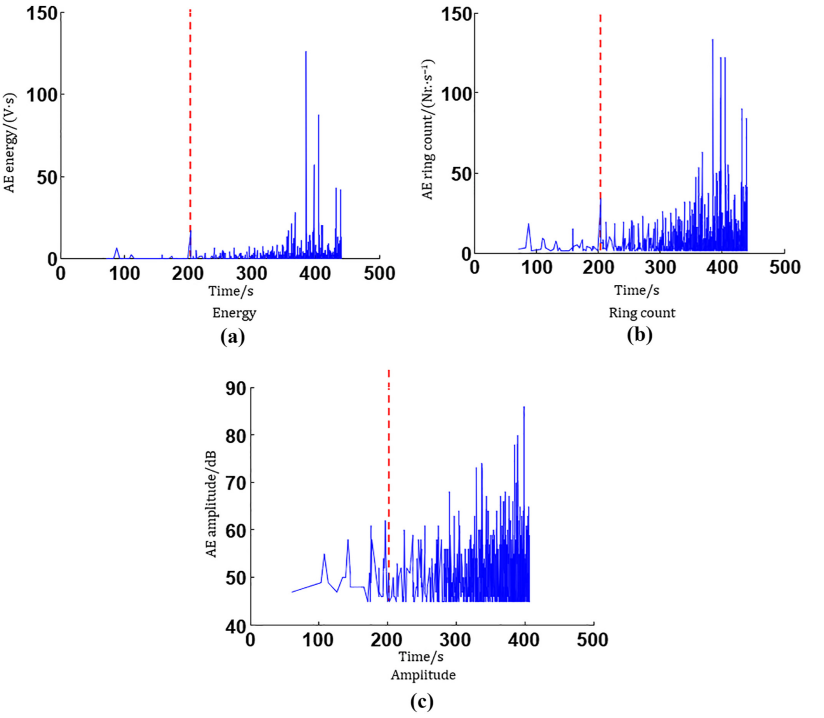

Figure 8.
Change curve of AE parameters (Sample 1)

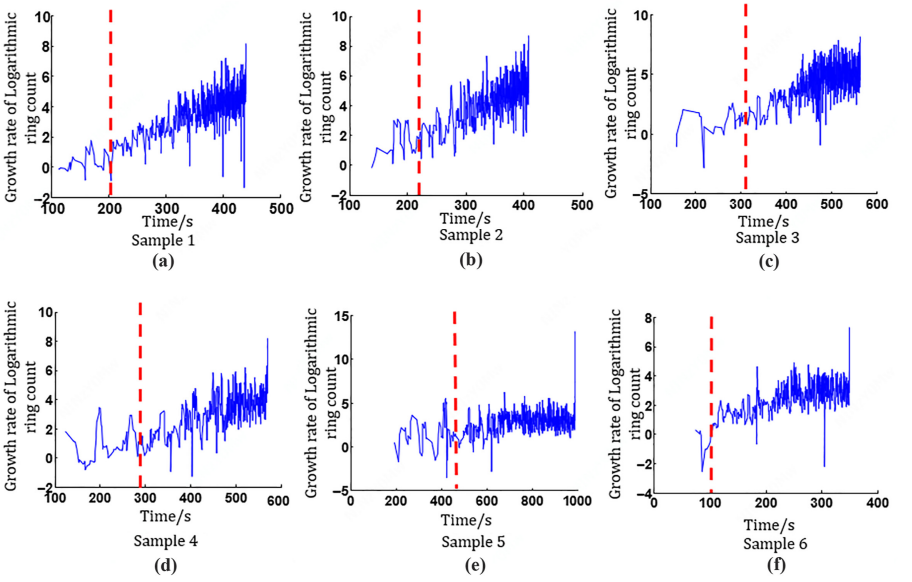

Figure 9.
Growth rate curves of logarithmic ring count

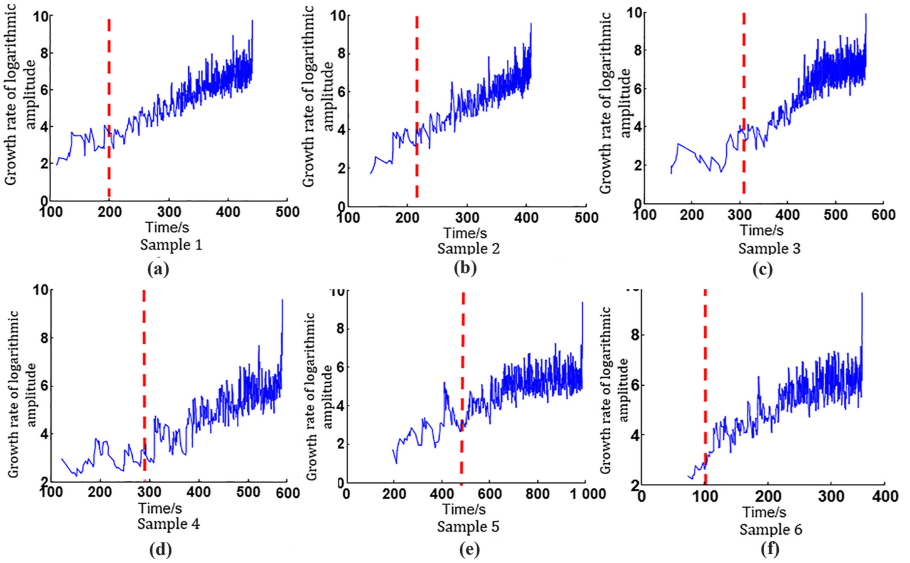

Figure 10.
Growth rate curves of logarithmic hit count

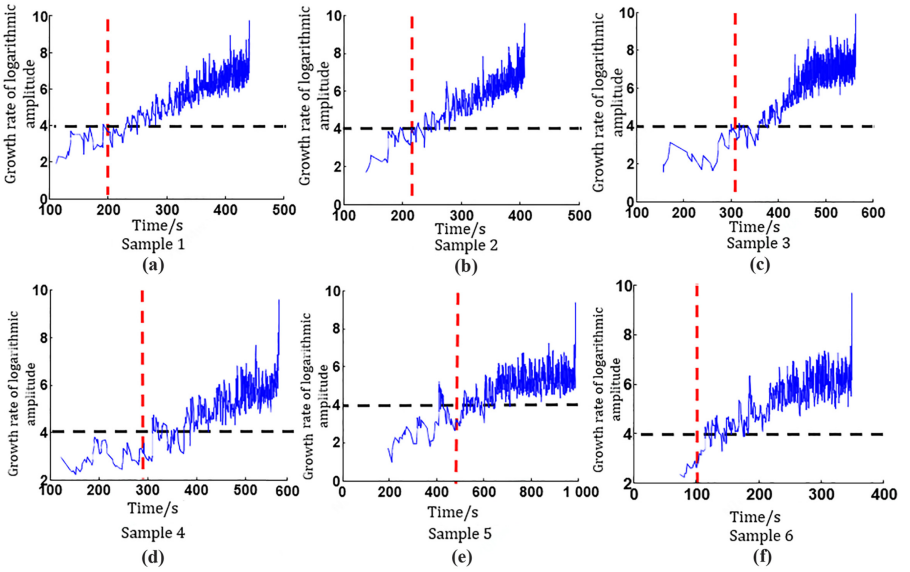

Figure 11.
Growth rate curves of logarithmic amplitude

According to the above analysis, it can be concluded that the growth rate of logarithmic hit count and that of the logarithmic amplitude can well reflect the damage stage of the material. Therefore, these two are selected as the characteristic parameters for the tensile damage of materials.

4.2 Damage identification by SVM classifier

SVM is a machine learning method proposed by Vapnik in 1995. It is based on VC (Vapnik–Chervonenkis) dimension and structural risk minimization of statistical learning theory and has the advantages of small samples, good generalization performance and global optimum (Cortes & Vapnik, 1995; Vapnik & Lerner, 1963). The paper introduces SVM algorithm to identify the damage of the HSR gearbox housing during the tensile process.

The SVM algorithm to identify the damage of the HSR gearbox housing during the tensile process is as follows.

(1) The growth rates of logarithmic hit count, logarithmic amplitude, hit count and amplitude are selected as the characteristic values to identify the damage stage of the sample.

(2) SVM classifier is used. The results of 5 of the 6 tensile tests are selected as the training sample, and the data of the remaining one are used as the test sample. The data are entered into SVM classifier as follows

$$\boldsymbol{Z} = (Z_1\, Z_2\, Z_3\, Z_4) \tag{3}$$

where

Z_1 – the growth rate of logarithmic hit count;

Z_2 – the growth rate of logarithmic amplitude;

Z_3 – the growth rate of hit count;

Z_4 – the growth rate of amplitude.

(3) The classification results to be entered are defined as −1 (safe stage) and 1 (early warning stage) depending on the stage of materials.

The identification and classification results of damage data in different stages by SVM algorithm are shown in Table 2.

It can be seen from Table 2 that the classification accuracy is fairly good in both safe and early warning stages, with 16 samples incorrectly classified.

The reason for the difference in classification accuracy is the imbalance of data. The data volume in safe stage is much smaller than that in the early warning stage. To resolve this issue, WSVM can be used for classification.

4.3 Damage identification by WSVM classifier

The concept of WSVM classifier is to assign different penalty coefficients to different categories of samples. If the classification accuracy of a category needs to be emphasized, a higher weigh λ_i may be assigned, and then its penalty coefficient C will become $\lambda_i C$. Many

Table 2. SVM classification results based on characteristic values extracted from this paper

Training data	Test data	Classification accuracy in safe stage	Classification accuracy in early warning stage
8,129 sets (219 sets in safe stage; 7,910 sets in early warning stage)	944 sets (57 sets in safe stage; 887 sets in early warning stage)	71.9% (41/57)	98.2% (871/887)

methods can be used to determine λ_i. In this paper, the weight of data in safe stage is defined as $\lambda_{-1} = 1$, and the weight of data in early warning stage is defined as $\lambda_1 = m_{-1}/m_1 = 0.028$, where m_{-1} is the data volume of the training sample in safe stage, and m_1 is the volume in early warning stage. The samples are entered into WSVM classifier in the same way as SVM classifier. The classification results are shown in Table 3.

The analysis shows that all the samples incorrectly classified are found in the transition stage. SVM classifier categorizes the transition data into the early warning stage, while WSVM classifier categorizes them into the safe stage. The incorrect classification may cause misinterpreting the safe stage as the early warning stage which, though guarantees operation safety, causes economic costs due to incidents including incorrect shutdown of equipment for maintenance. Generally speaking, the WSVM classifier is superior to the SVM one especially in the aspect of operation safety.

5. Life prediction based on degradation data

5.1 Extraction of degradation data

The test results show that the growth rates of the hit count and amplitude follow a monotonic increasing trend, and their characteristic values at the time of failure are basically consistent. Given that they reflect the damage stage of the material concerned, the two characteristic values can be used in the degradation curve. The growth rate curve of hit count is basically consistent with that of the amplitude, so the growth rate of hit count is used to quantify the performance degradation. The growth rate curves of logarithmic hit count are shown in Figure 12, where, the dotted line is the centroid curve, describing the overall trend of the curve, that is, the degradation of material performance.

Figure 12 shows that fracture occurs when the growth rate of hit count goes around 6. A close observation of the curves' characteristics indicates that the degradation trajectory follows a linear or a quadratic pattern, but further verification is required.

Once the material enters the yield stage, it enters the unsafe stage and needs to be replaced. But in fact, it takes some time for the gearbox housing material to fracture after it enters the yield stage. If the degradation trajectory of the gearbox housing material, or in other words the life prediction model, can be fitted according to the data of the safe stage, the remaining life of the material can be predicted. In this way, the damage of the material can be quantified, providing references to the maintenance and replacement of the material.

5.2 Building of degradation model

The degradation model is built based on the data obtained in the safe stage of the tensile test. According to the variation law of the curve, linear equation and quadratic curve equation are selected from the commonly used degradation curve models to fit. The fitting results are shown in Figures 13 and 14 where red curves are the fitted curves.

It can be concluded from Figure 13 that in the fitting results, sample 5 and 6 show good results in linear fitting, followed by sample 2, but significant errors are noticed in case of sample 1, 3 and 4.

Table 3. WSVM classification results based on characteristic values extracted from this paper

Training data	Test data	Classification accuracy in safe stage	Classification accuracy in early warning stage
8,129 sets (219 sets in safe stage; 7,910 sets in early warning stage)	944 sets (57 sets in safe stage; 887 sets in early warning stage)	100% (57/57)	94.1% (835/887)

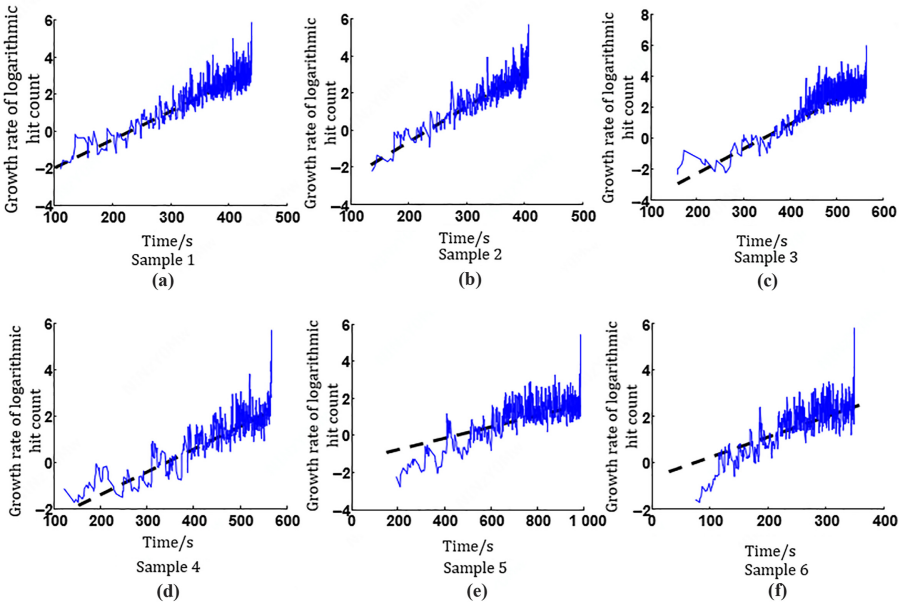

Figure 12.
Curves of logarithmic hit count growth rates

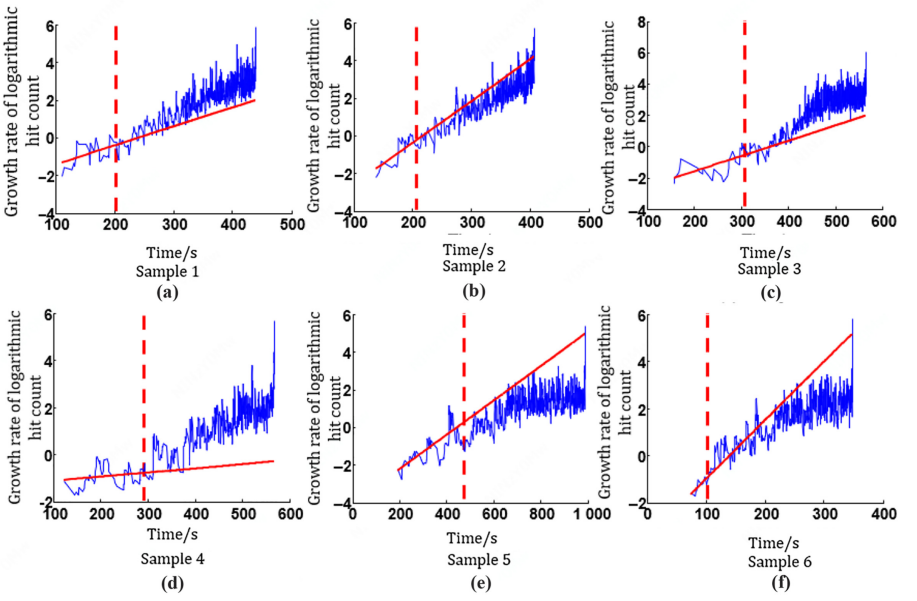

Figure 13.
Results of linear fitting

The significant errors noticed in the direct fitting of the growth rate curves of logarithmic hit count for samples 1, 3 and 4 can be explained by the fact that the characteristic values change only mildly in the safe stage, and then vary significantly in the early warning stage.

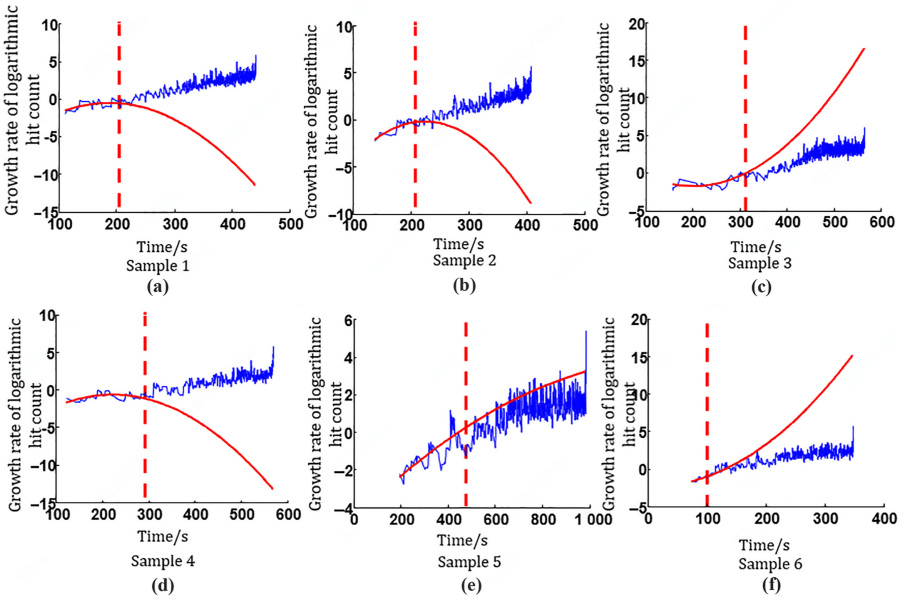

Figure 14.
Results of quadratic curve fitting

Therefore, the data in the safe stage are insufficient to characterize the variation law in the early warning stage.

Figure 14 shows that sample 5 shows good results in quadratic curve fitting, while major errors are found in other samples. Given that the variation law can hardly be characterized, the model is not suitable for the study.

This paper finds that key peaks generally follow a linear pattern, therefore it selects the peaks along the increasing trend amid the safe stage for linear fitting, and the results are shown in Figure 15. In the figures, red curves are the fitted curves.

It can be seen from Figure 15 that the results of peak linear fitting are better than those of linear fitting and quadratic curve fitting, but for some samples, sample 3 and 5 for instance, errors of the fitting results are quite significant. In the case of sample 3, only limited number of peaks is found in the safe stage resulting in inaccuracy of modeling; while for sample 5, a high peak in the safe stage makes the degradation curve too conservative to be a valuable reference.

5.3 Life prediction results and analysis

According to the characteristics of each degradation curve in Figure 15, the fracture threshold of samples is determined as 5.8, and the calculation formula of prediction error E' is

$$E' = \frac{|T_p - T_r|}{T_r} \times 100\% \tag{4}$$

where

T_p – the predicted life;

T_r – the actual life.

The prediction results and prediction errors are shown in Table 4.

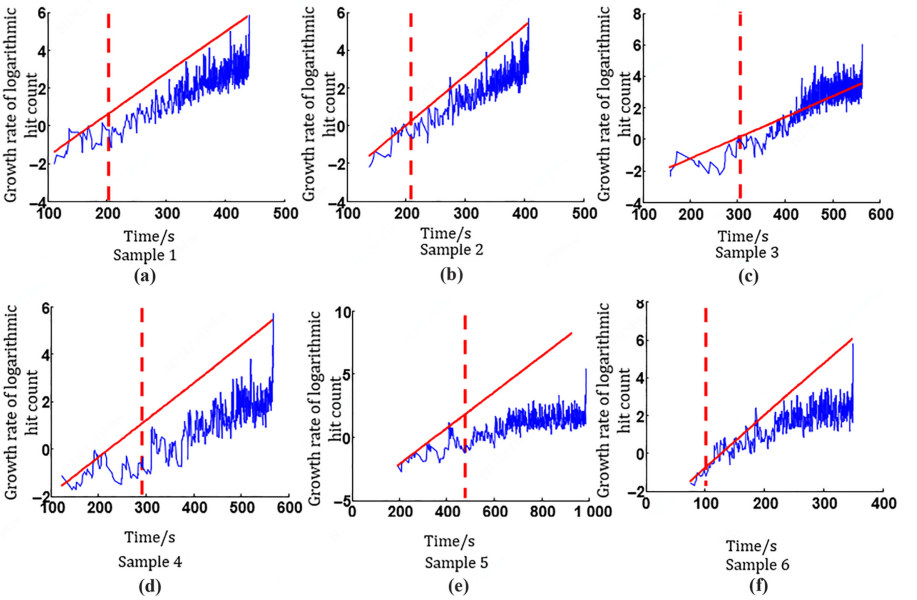

Figure 15.
Results of peak linear fitting

Sample	Prediction result/s	Prediction error/%
1	440.106 1	0.08
2	423.261 9	3.70
3	738.796 1	31.00
4	593.391 1	4.40
5	763.522 5	22.60
6	340.773 8	2.40

Table 4.
Results of peak linear fitting

Table 4 shows that samples 3 and 5 show significant prediction errors, while in the case of other samples, the errors are very small.

Again, significant errors noticed in samples 3 and 5 can be explained by the fact that in the case of sample 3, only limited number of peaks are collected, while in the case of sample 5, major peak is found in the safe stage. Despite of large errors in the life prediction results of some tensile samples, the method is still of reference to life prediction. It needs to be noted though more tests are required to verify the feasibility of this method.

6. Conclusions

(1) The analysis of AE signals acquired in the tensile tests of the gearbox housing material shows that the logarithmic growth rate of AE signals can help indicate which stage of the gearbox housing material is in during the tensile process.

(2) Based on the characteristics of AE signals during the tensile test process, this paper uses SVM classifier for damage identification and classification of the characteristic

parameters extracted, while the WSVM algorithm is used to improve the classifier. The approach greatly reduces misinterpretation of the early warning stage (as the safe stage) and improves the classification accuracy to above 94%, realizing the real-time nondestructive damage identification of the HSR gearbox housing material in the tensile process.

(3) As this paper looks into the relationships between characteristic values and the tensile life, it builds up the degradation model of the gearbox housing material during the tensile process, which helps predict the service life remained. The results verified the feasibility of the model, providing new concepts for the life prediction of tensile samples.

References

Andreykiv, O., Skalsky, V., Serhiyenko, O., & Rudavsky, D. (2010). Acoustic emission estimation of crack formation in aluminium alloys. *Engineering Fracture Mechanics*, *77*(5), 759–767.

Bhuiyan, M. S. H., Choudhury, I. A., Dahari, M., Nukman, Y., & Dawal, S. Z. (2016). Application of acoustic emission sensor to investigate the frequency of tool wear and plastic deformation in tool condition monitoring. *Measurement*, *92*, 208–217.

Cortes, C., & Vapnik, V. (1995). Support-vector networks. *Machine Learning*, *20*(3), 273–297.

Dong, X. (2007). *The working principle and structural characteristics of high speed EMUs*. Beijing: China Railway Publishing House (in Chinese).

Griffin, J. M., Shanbhag, V. V., Pereira, M. P., & Rolfe, B. F. (2021). Application of machine learning for acoustic emissions waveform to classify galling wear on sheet metal stamping tools. *The International Journal of Advanced Manufacturing Technology*, *116*(1/2), 579–596.

Hamdi, S. E., Le, D. A., Simon, L., Plantier, G., Sourice, A., & Feuilloy, M. (2013). Acoustic emission pattern recognition approach based on hilbert-huang transform for structural health monitoring in polymer-composite materials. *Applied Acoustics*, *74*(5), 746–757.

Huang, Z., Liu, Y., Mao, H., Wang, X., Li, X., & Mao, H. (2017). Feature analysis for acoustic emission signals during metal fatigue damage based on Kolmogorov entropy and correlation dimension. *Journal of Vibration and Shock*, *36*(15), 210–214 (in Chinese).

Li, X., Luo, G., Long, S., Chen, G., & Li, Q. (2016). Location method of acoustic emission by time reversal focusing and enhancing for steel plate. *Chinese Journal of Scientific Instrument*, *37*(8), 1792–1799 (in Chinese).

Melnikov, B. F., Averin, P. I., & Melnikova, E. A. (2019). Intelligent processing of acoustic emission data based on cluster analysis. *Journal of Physics: Conference Series*, *1236*(1), 012044.

Roder, G. J., Guerrero-mata, M. P., & Colás, R. (2003). Crack propagation in a hard-faced AISI type 304 stainless steel. *Materials Characterization*, *51*(2/3), 95–99.

Shi, H., Li, H., Wang, Z., & Pan, Q. (2019). Acoustic emission signal processing technology based on wavelet packet energy spectrum. *Journal of Test and Measurement Technology*, *33*(3), 201–208 (in Chinese).

Vapnik, V. N., & Lerner, A. Y. (1963). Recognition of patterns with help of generalized portraits. *Avtomat. i Telemekh.*, *24*(6), 774–80.

Wang, X., Zhu, C., Mao, H., & Huang, Z. (2010). Source location of cracks in a turbine blade based on kernel principal component analysis and support vector machines. *Journal of Vibration and Shock*, *29*(11), 226–229, 264 (in Chinese).

Wang, W., Zang, Y., Qu, J., Li, G., & Dai, X. (2018). Dynamic stress response and fatigue reliability of gearbox housing for G-series high speed train. *China Railway Science*, *39*(6), 90–97 (in Chinese).

Yao, X., Zhang, Y., Ming, T., & Liu, S. (2010). Application of support vector machine and acoustic emission to fault diagnosis of gear crack. *Journal of Naval University of Engineering*, *22*(2), 70–73, 112 (in Chinese).

Yoshida, K., Tokuyama, Y., Yasuhara, Y., & Nishino, H. (2012). Evaluation of AE sources during tensile deformation of Al-Mg-Si alloys with different heart treatment. *30th European Conference on Acoustic Emission Testing and 7th International Conference on Acoustic Emission* Granada: University of Granada.

Corresponding author
Zhang Weidong can be contacted at: zwdpaper@163.com